In vivo liver differentiation by ultrasound using an artificial neural network

D. Zatari and N. Botros
Department of Electrical Engineering, Southern Illinois University, Carbondale, Illinois 62901

F. Dunn
Bioacoustics Research Laboratory, Department of Electrical and Computer Engineering, University of Illinois at Urbana-Champaign, Urbana, Illinois 61801

(Received 27 August 1993; accepted for publication 16 March 1994)

A pattern recognition algorithm and instrumentation for *in vivo* ultrasound human liver differentiation are presented. An available 16-MHz microprocessor-based data acquisition and analysis system with 6-bit resolution is used to capture, digitize, and store the backscattered ultrasound signal. The algorithm is based on a multilayer perceptron neural network using the backpropagation training procedure. The network is implemented to differentiate between normal and abnormal liver. Data earlier obtained from 18 volunteers with normal liver history and from 12 volunteers with liver abnormalities are used to test the algorithm. The power spectra of the backscattered signal from depths of 5, 6.5, and 8 cm in the liver are calculated. The acoustic attenuation coefficient is calculated by the log spectral difference technique over the frequency range from 1.5 to 4.5 MHz. The change of speed of sound with frequency (dispersion) is estimated over the 3-MHz bandwidth. The attenuation and velocity dispersion are used as differentiation features. The results show that of the 22 tested cases, the system differentiated correctly 19 and 20 cases when using the attenuation and the velocity dispersion, respectively. The average magnitude of dispersion of liver is estimated to be 1.67 ± 0.1 m/s/MHz and about 2.3 ± 0.18 m/s/MHz in the normal and abnormal cases, respectively. The overall performance of the system for liver differentiation is 91% for normal cases, and 86% for abnormal cases. The data files are also differentiated using the nearest neighbor statistical classifier. The results show that of the 30 tested cases, 23 files are differentiated correctly using the attenuation coefficient.

PACS numbers: 43.35.Wa, 43.80.Vj

INTRODUCTION

Ultrasound imaging has proved to be a powerful tool in characterizing the state of soft tissues, such as human liver;[1] for medical diagnostic purposes; it is noninvasive and considered safe. Most conventional ultrasound imaging instruments present two-dimensional images based mainly upon the amplitude of the returned rf signal.[2] The brightness of the pixels comprising the image is a function of the amplitude of the backscattered signal. By observing the brightness and the texture of the image, the radiologist can determine whether or not the tissue is normal. However, in some cases it may be difficult to diagnose the tissue from this image alone, and a biopsy examination must be conducted. This image, moreover, may not provide definitive information about the type of abnormality present. During the past decade, with recent advances in computer technology, application of quantitative analysis of the ultrasound backscattered signal from soft tissues has accelerated. This quantitative analysis often includes feature extraction from the signal, followed by a pattern recognition algorithm to diagnose the state of the tissue. Several investigators[3–6] have reported reasonable success in diagnosing disorders of liver, using such analytic methods. The pattern recognition algorithms employed are mainly Bayes and nearest-neighbor statistical classifiers.

The goal of the present study is to enhance the capability of diagnosing disorders of tissues and organs. The approach taken involves analyzing quantitatively the backscattered signal and applying a powerful pattern recognition technique based on artificial neural networks. The neural network approach has been employed by several investigators to characterize soft tissues.[7–11] It is also reported that the performance of the network outperforms the traditional statistical classifiers such as the nearest-neighbor and the linear discriminant analysis.[8,11]

It is evident that the method employed by these investigators was based on extraction features from an image, whereas in this study, features are extracted from the acoustic parameters of the signal.

This method of interrogating the tissue is believed to be easier than visual interpretation of the time domain B-scan image (see Fig. 1).[4,5,12] Accurate results may preclude the need for biopsy examination.

I. THEORETICAL ANALYSIS

A. Estimation of the attenuation coefficient for human liver

The acoustic attenuation coefficient $\alpha(f)$ in the frequency domain can be written as[3,4,13]

$$\alpha(f)=\frac{1}{2(x_2-x_1)}\ln\left(\frac{E_r(x_1,f)}{E_r(x_2,f)}\right), \tag{1}$$

 0001-4966/94/96(1)/376/6/$6.00

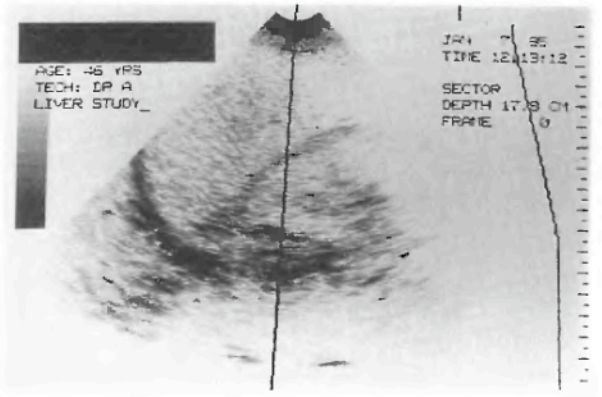

FIG. 1. A B-scan image of human liver.[3]

where $E_r(x_1,f)$ and $E_r(x_2,f)$ represent the power spectra of the backscattered signal from depths x_1 and x_2, respectively, with x_1 different than x_2. Equation (1) indicates that calculation of $\alpha(f)$ depends on the difference between two far-zone depths.

Empirically, the attenuation coefficient has been found to be expressible in terms of frequency as[1,4,14]

$$\alpha(f)=a\cdot f^b, \tag{2}$$

where a and b are tissue absorption constants. It is reported that for normal liver, a has values around 0.5 dB/cm/MHz while advanced cirrhotic liver may produce values as high as 0.9.[15] The value of b is about 1.1 to 1.2 for liver in the low megahertz frequency range and can reach 2 for high frequencies.[14]

B. Estimation of velocity dispersion in human liver

Ultrasonic dispersion is difficult to measure accurately in soft tissue, because of its relatively small value and because methods of high accuracy are generally not available.[1,14] However, dispersion can be estimated from knowledge of the attenuation coefficient. Since an acoustic medium may be represented as a causal linear system, the real and imaginary parts of the frequency-dependent dynamic compressibility are related by the Kramers–Kronig relationships.[16] Based on this fact, the nearly linear relationships between attenuation and dispersion can be expressed in an approximate form as[16]

$$\alpha(\omega)=\frac{\pi\omega^2}{2c_0^2}\cdot\frac{dc(\omega)}{d\omega}. \tag{3}$$

By integrating Eq. (3) over the frequency range ω_0 to ω, the phase velocity $c(\omega)$ can be expressed as

$$c(\omega)=c_0+\frac{2c_0^2}{\pi}\int_{\omega_0}^{\omega}\frac{\alpha(\omega)}{\omega^2}\,d\omega, \tag{4}$$

where c_0 is the sound velocity at a convenient reference frequency ω_0 and ω is the maximum frequency encountered. The dispersion is also expressed as

$$\delta c(\omega)=c(\omega)-c_0. \tag{5}$$

Usually, $\delta c(\omega)$ is much less than c_0. The approximation is due to the fact that the magnitude of the dispersion is small. By using Eqs. (1), (4), and (5), the dispersion can be written as

$$\delta c(\omega)=\frac{2c_0^2}{\pi}\cdot\frac{1}{2dx}\cdot\sum_{\omega_0}^{\omega}\frac{1}{\omega^2}\ln\left(\frac{E_r(x_1,f)}{E_r(x_2,f)}\right)\Delta\omega. \tag{6}$$

According to Eq. (4), if the attenuation varies linearly with frequency, the incremental increase in speed $\delta c(\omega)$ should vary logarithmically over the defined frequency range. Equations (4) and (6) are used to estimate the magnitude of dispersion for further investigation.

II. DATA ACQUISITION SYSTEM

The power spectrum of the ultrasound backscattered signal should be measured to determine the attenuation coefficient. A high speed data acquisition and analysis system with sampling rate 16-MHz and 6-bit resolution was used to capture, digitize, and store the signal from different depths of the liver specimen. The digitized data are transferred to a personal computer where attenuation and velocity dispersion are calculated. The system was coupled to an ultrasound diagnostic machine. Figure 2 is a simplified block diagram of the

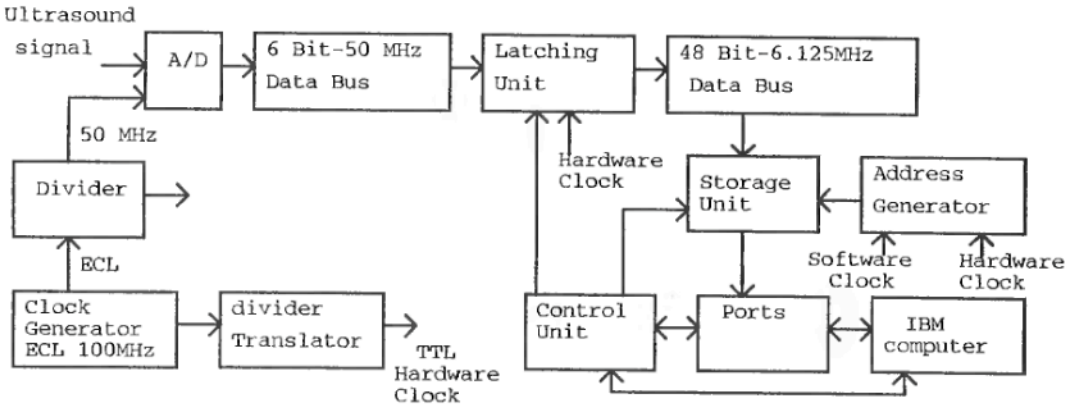

FIG. 2. Block diagram of the system.

TABLE I. Liver data.

Number of subjects	Liver condition
18	Normal
2	Fatty infiltration
3	Hepatitis
5	Cirrhosis
2	Fibrosis

system. Details of the system have been published elsewhere.[3]

III. DATA PROCESSING

In order to test the hypotheses culminating in Eqs. (1) and (6), the data of Botros[3] were employed. These data were collected from 18 normal liver subjects and 12 abnormal liver subjects (see Table I). Normality and abnormality were determined by using an ATL (Advanced Technology Laboratory) clinical ultrasound diagnostic instrument MK-500 B-scanner, having a 3-MHz center frequency; abnormalities were confirmed by biopsy examination. The user examined each patient with a two-dimensional modality under the routine clinical protocols to select the area of interest and the depth. Data were collected from different depths of 5, 6.5, and 8 cm. A sampling window, predetermined to be 32 μs (approximately equivalent to 4.8 cm of liver tissue), allowed the digital data to be gathered during this time interval. At each depth, and for every collection cycle, the backscattered signal was sampled eight times and stored in eight files on the microcomputer. Each file contained 512×6 bits of data; the total number of files per case at this stage was 24 (8 replications×3 depths=24 files).

A fast Fourier transform (FFT) is applied to the 512 data points, and the power spectrum is calculated. The frequency range extends from 0 to 8 MHz. Frequencies less than 1.53 MHz, or greater than 4.5 MHz, have very small amplitudes and hence these components are filtered out. After digital filtering is performed on each file, the data points per file are reduced to 99. Theoretically, the data in the eight files for each subject should be identical but, in fact, they are found to be slightly different due to the statistical nature of the backscattered signal, and due to system noise. To minimize the discrepancy among the eight files representing the same subject, histograms are formed from these files with each interval (0.1188 MHz) representing the average value of four consecutive data points. This process reduced the number of data points of each file to 25. Figure 3 shows examples of the power spectrum for a subject with normal liver and for one with a diseased liver.

IV. ESTIMATION OF ATTENUATION AND VELOCITY DISPERSION

The measured power spectra of the backscattered signal are used to calculate the acoustic attenuation coefficient using the log spectral difference approach, as given by Eq. (1). The attenuation is calculated for each file from depths of 5 and 6.5 cm, and from depths of 6.5 and 8 cm. Averaging is performed on every four adjacent data points of each spectrum and one file for each subject representing the average attenuation coefficient is finally obtained. The total number of files (subjects) are 18 normal and 12 abnormal; each file consisting of a vector of 25 points that represents the attenuation as a function of frequency. Figure 4 shows the average attenuation coefficient as a function of frequency for a normal and an abnormal liver specimen.

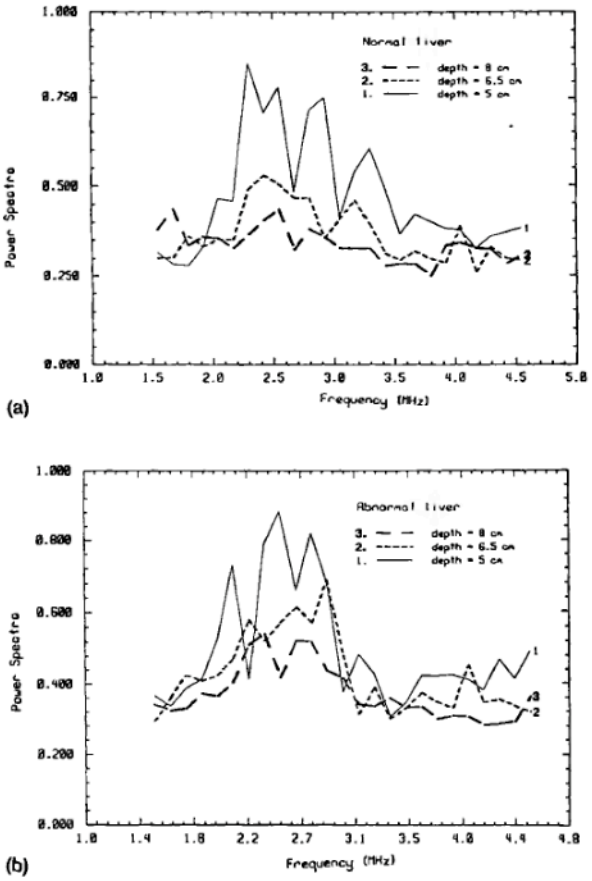

FIG. 3. (a) Average power spectrum versus frequency for normal liver specimens. (b) Average power spectrum versus frequency for abnormal liver specimens.

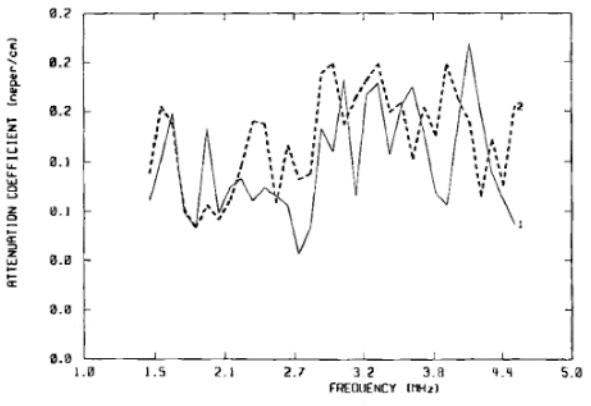

FIG. 4. Average attenuation coefficient versus frequency for (1) normal and (2) abnormal liver specimens.

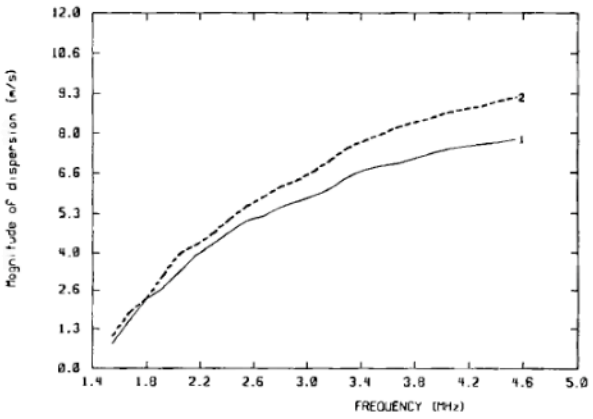

FIG. 5. Average ultrasound velocity dispersion versus frequency for (1) normal and (2) abnormal liver specimens.

The change of the speed of sound with frequency for each subject is estimated by using Eq. (6) over the defined frequency range. Evidence exists in the literature to suggest that the speed of sound in tissue can vary with the pathological condition, and that the pathology-related changes in the speed of sound are very small.[18] The velocity dispersion is estimated for the 30 files in a similar manner as the attenuation. Figure 5 shows the calculated change of speed of sound with frequency for a normal and for an abnormal liver specimen.

V. DIFFERENTIATION ALGORITHM

A computer program was written to perform the analysis described in previous sections. Figure 6 [Fig. 6(a), overall system algorithm; Fig. 6(b), differentiation algorithm] shows the flowchart of the software program implemented for liver differentiation. The algorithm is based primarily on the use of the neural network as a pattern classifier.

VI. THE ARTIFICIAL NEURAL NETWORK

Neural networks have been used in a wide range of signal processing and pattern recognition applications and have been applied successfully in such diverse fields as speech processing and control applications. Their attractiveness lies in the relative simplicity with which the network can be trained for a specific problem, along with their ability to perform nonlinear data processing. A feed-forward network with one hidden layer of size 7 nodes (see Fig. 7) is chosen for its relative simplicity and power. The number of nodes of the hidden layer is determined by trial and error to ensure rapid convergence of the network during training. As pointed

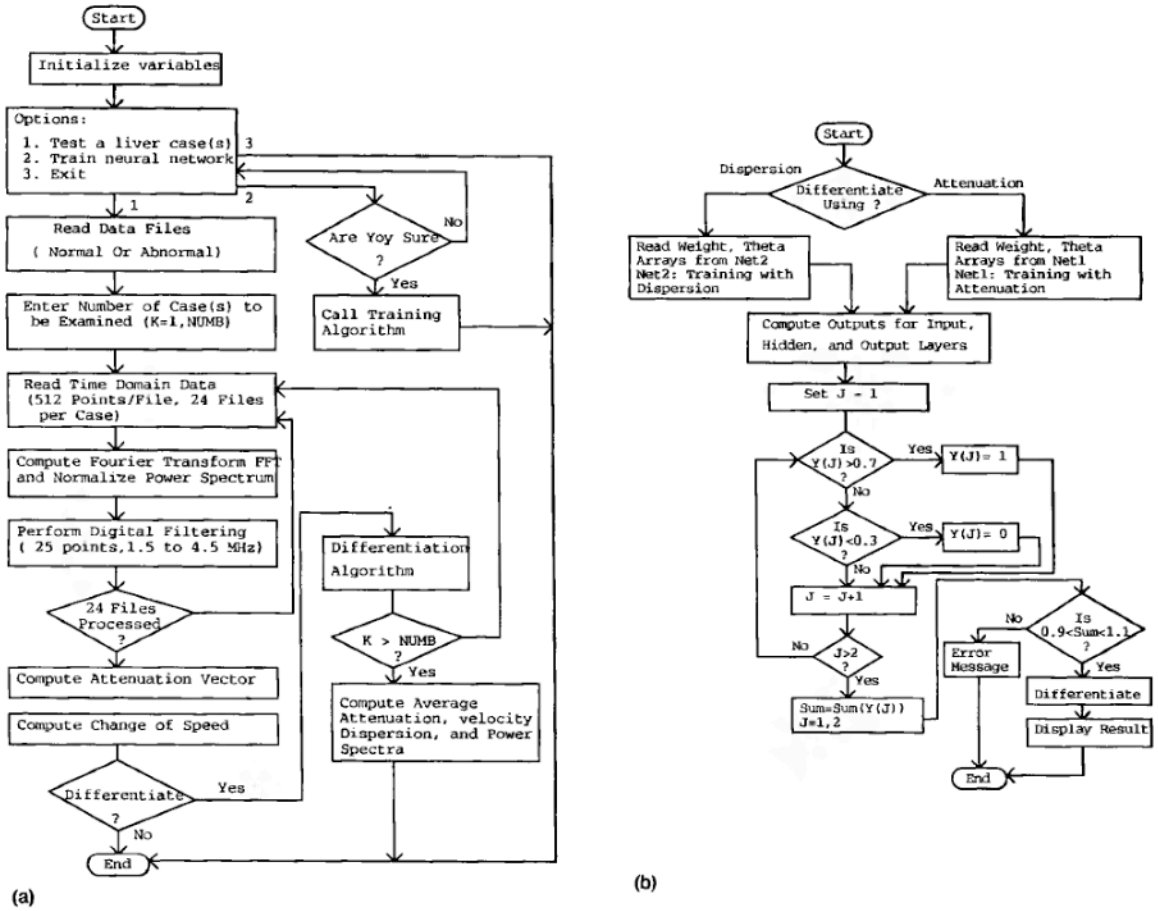

FIG. 6. (a) Overall system algorithm. (b) Differentiation algorithm.

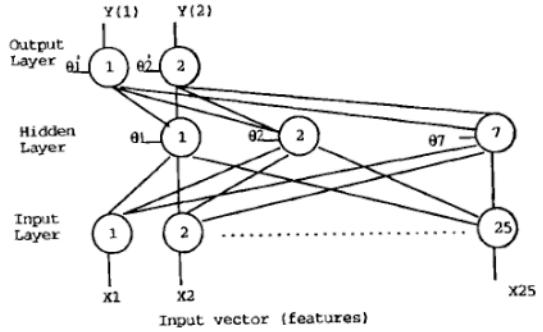

FIG. 7. The artificial neural network.

out by Lippman,[19] such a network is capable of producing a wide range of nonlinear mappings including any possible unbounded convex regions in the space spanned by the inputs. The network is used to differentiate among the states of liver, which would be normal or abnormal. The input to the network is a continuously valued vector $x_1, x_2, \ldots, x_{25}$ representing either the attenuation coefficient or the change of speed (dispersion) of the backscattered signal. The backpropagation algorithm is used for training the network. The output of the network is the class of the current input, normal or abnormal liver. The output of node j, y_j is computed as follows

$$y_j = g\left(\sum w_{ij} x_i - \theta_j\right), \tag{7}$$

where θ_j is the offset (bias) of node j, w_{ij} is the weight of the connection between node j and node i, and the function g is the sigmoid nonlinearity

$$g(\gamma) = 1/(1+e^{-\gamma}). \tag{8}$$

The network is trained using the delta rule with momentum as follows:[19]

(1) Initialize the weights and offsets. Each node, except the input nodes, is assigned to an initial offset. The input nodes have no offset; they act as buffers.

(2) Starting from the output layer and going backward to the input layer, adjust offsets recursively until the weights are stabilized. The weights and offsets are adjusted by using the formulas

$$w_{ij}^{\text{new}} = w_{ij}^{\text{old}} + \mu \epsilon_j x_i, \tag{9}$$

$$\theta_j^{\text{new}} = \theta_j^{\text{old}} + \mu \epsilon_j, \tag{10}$$

where μ is the gain factor and is assumed to be 0.5 and ϵ_j is the error. The weights are considered stabilized if the value of each new weight is 99% of its previous value. If node j is an output node, then

$$\epsilon_j = y_j(1-y_j)(d_j - y_j), \tag{11}$$

where d_j is the desired output of node j, and y_j is the actual output. The desired output for all output nodes is set to either 0 or 1. If node j is a hidden node, then

$$\epsilon_j = y_j(1-y_j)\sum_k \epsilon_k w_{jk}, \tag{12}$$

where k runs over all nodes in the layers above node j.

The training set for the network consists of eight vectors each of 25 data points. The eight vectors (files) are selected from four files representing normal liver subjects, and four files each representing a single type of abnormality (see Table II). Due to the limited data employed in this study, eight files (four normal and four abnormal) have been used as a training set. However, it is recommended to use a larger number of files (if it is available) to lower the sparseness of the training data. The desired output was set to produce an output vector (1,0) for normal cases, and (0,1) for abnormal cases and otherwise for unclassified cases. After training is completed, any arbitrary vector, either for the attenuation or for the change of sound speed with frequency, can be applied as an input to the network for differentiation purposes.

TABLE II. Classification results.

Liver condition	Files for training	Files for testing	Network output (passed files) atten.	disp.
Normal	4	14	13	14
Abnormal	4	8	6	6

VII. RESULTS

The files used in the training were not included in the test set. The test set for the network consisted of 14 normal and eight abnormal files. Data stored in these files were processed and the two classes (normal and abnormal) were predicted by the network. These classes were compared to the previously known ones. The results show that of the 22 tested cases, the system diagnosed correctly 19 and 20 cases, when using attenuation and dispersion, respectively. The time-domain data and the power spectra of the failed files are visually inspected and compared with the other files. After conducting simple statistical calculations for the mean and variance, it is found that the failed files are corrupted with noise. This noise may be generated by the system and/or interference of the examiner by shaking his/her hand while holding the transducer. The average dispersion in normal liver was found to be 1.67 ± 0.1 m/s/MHz and in the abnormal cases about 2.3 ± 0.18 m/s/MHz. These findings are in agreement with those observed by others.[16,20] Figures 4, 5, and 6 are examples of the variations with frequency of the average power spectra, the attenuation coefficient, and the dispersion, respectively, for a normal liver and an abnormal liver specimen.

The results indicate that the percent of success is 86 using attenuation and 91 using velocity dispersion. Testing accuracies of 81.2% and 90.6% have been reported when applying two commercial neural network packages to discriminate among normal and abnormal liver textures.[11]

Further examination for the data files are made using a statistical nearest-neighbor classifier as reported in Ref. 3. The results show that of the 30 cases tested, the algorithm differentiated correctly 23 cases using attenuation.

VIII. CONCLUDING REMARKS

The attenuation coefficient has been used to estimate the dispersion in human liver tissue. According to Eq. (6), the nearly linear dependence of the attenuation coefficient on frequency for normal and abnormal liver specimens leads to the prediction of nearly logarithmic frequency dependence for the dispersion. The numerical value of the average change in phase velocity in the frequency range 1.5 to 4.5 MHz is 1.67 ± 0.1 m/s/MHz for normal liver and 2.3 ± 0.18 m/s/MHz for abnormal liver specimens. To some extent, these values are in agreement with the findings of other investigators.[16,20] For soft tissues, the average speed is often assumed to be 1540 m/s with a small variation mainly due to fluctuation in elasticity rather than density. However, from a practical point of view, the speed of sound in soft tissues is not a strong function of frequency.[1] Consequently, the dispersion anticipated in normal and abnormal liver is very small. Hence, without loss of generality, it can be claimed that dispersive effects on liver are correspondingly negligible. This conclusion is also supported by Kuc.[15] The calculated quantities of attenuation and dispersion are used to identify liver pathologies. Despite the fact of small dispersion, it is shown in this study that the magnitude of dispersion can be used as a useful discriminator. The results obtained for the estimated attenuation coefficient and the dispersion using this scheme and for the cases examined, suggest that *in vivo* human liver differentiation for normal and abnormal states can be achieved. Comparing the results obtained using the neural network with those obtained using the nearest-neighbor algorithm, show that the neural network outperforms this traditional statistical classifier. This has also been observed by others.[7,8,11] Further studies should investigate differentiation among different liver pathologies. This can be accomplished by acquiring a much larger set of data representing a variety of the abnormal cases.

ACKNOWLEDGMENT

F. Dunn acknowledges the support of the National Institute of Health.

[1] J. C. Bamber and M. Tristan, "Diagnostic ultrasound," *The Physics of Medical Imaging*, edited by S. Webb (Adam Hilger, New York, 1988), pp. 319–388.

[2] J. F. Havlice and J. C. Taenzer, "Medical Ultrasonic Imaging: An Overview of Principles and Instrumentation," Proc. IEEE **67**(4), 620–641 (1979).

[3] N. M. Botros, "A High Speed Data Acquisition and Analysis System for Ultrasonic Energy Measurements," IEEE Trans. Instrum. Meas. **37**(4), 515–518 (1988).

[4] D. Nicholas, "Evaluation of backscattering coefficients for excised human tissues: Results, interpretation and associated measurements," Ultrasound Med. Biol. **8**(1), 7–15 (1982).

[5] B. S. Garra, M. F. Insana, T. H. Shawker, and M. A. Russel, "Quantitative estimation of liver attenuation and echogenicity: Normal state versus diffuse liver disease," Radiology **162**, 61–67 (1987).

[6] M. F. Insana, R. F. Wagner, and B. S. Garra, "Supervised pattern recognition techniques in quantitative diagnostic ultrasound," in International Symposium on Pattern Recognition and Acoustical Imaging **768**, 146–154 (1987).

[7] J. S. Ostrem, A. D. Valdes, and P. D. Edmonds, "Application of Neural Nets to Ultrasound Tissue Characterization," Ultrason. Imag. **13**, 298–299 (1991).

[8] G. Schmitz, M. Kruger, and H. Ermert, "Comparison of a Neural Network and a *K*-Nearest Neighbor Classifier for the Classification of Different Scatterer Densities," Ultrason. Imag. **15** (2), 168 (1993).

[9] M. S. Klein Gebbinck, J. T. M. Verhoven, J. M. Thijssen, and T. E. Schouten, "Application of Neural Networks for the Classification of Diffuse Liver Disease by Quantitative Echography," Ultrason. Imag. **15**(2), 168–169 (1993).

[10] A. S. Hayrapetian, K. K. Chan, W. S. Weinberg, and E. G. Grant, "Neural Network for Ultrasound Image Segmentation," Ultrason. Imag. **15**(2), 169 (1993).

[11] J. S. DaPonte and P. Sherman, "Classification of Ultrasonic Image Texture by Statistical Discriminant Analysis and Neural Networks," Comput. Med. Imag. Graphics **15**(1), 3–9 (1991).

[12] E. Walach, A. Shmulewitz, Y. Itzchak, and Z. Heyman, "Local tissue attenuation images based on pulsed-echo ultrasound scans," IEEE Trans. Biomed. Eng. **36**, 211–221 (1989).

[13] K. J. Parker and R. C. Waag, "Measurement of Ultrasonic Attenuation within Regions Selected from B-Scan Images," IEEE Trans. Biomed. Eng. **30**(8), 431–437 (1983).

[14] F. Dunn, P. D. Edmonds, and W. J. Fry, "Absorption and dispersion of ultrasound in biological media," in *Biological Engineering*, edited by H. P. Schwan (McGraw-Hill, New York, 1969), pp. 205–332.

[15] R. Kuc, "Clinical application of ultrasound attenuation coefficient estimation technique for liver pathology characterization," IEEE Trans. Biomed. Eng. **BME-27**, 312–319 (1980).

[16] M. O'Donnell, E. T. Jaynes, and J. G. Miller, "Kramers–Kronig relationship between ultrasonic attenuation and phase velocity," J. Acoust. Soc. Am. **69**, 696–701 (1981).

[17] N. M. Botros, "A PC-Based Tissue Classification System Using Artificial Neural Networks," IEEE Trans. Instrum. Meas. **41**(5), 633–638 (1992).

[18] T. Lin, J. Ophir, and G. Potter, "Correlation of sound speed with tissue constituents in normal and diffuse liver disease," Ultrason. Imag. **9**, 29–40 (1987).

[19] R. Lippmann, "An Introduction to Computing with Neural Nets," IEEE ASSP Mag. **4**, 4–22 (1987).

[20] P. K. Bhagat, M. P. Kadaba, V. N. Gupta, and V. C. Wu, "Microprocessor-based system for ultrasonic tissue characterization," Med. Instrum. **14**, 220–224 (1980).